Referee #2

This paper studies the effect of time variations in fossil fuel emissions on simulated CO2 concentrations. The paper does not use atmospheric observations and earlier papers have studied the subject to some extent. Nevertheless, the paper provides a nice addition to earlier studies and quantifies and compares the effects of time variations to rectifier effects expected from biosphere CO2 uptake and extends the subject to total column CO2 measurements (for which the effects are understandably less pronounced). I have little remarks about the paper, although at some points the results need to be checked carefully by the authors.

We have carefully checked the results. Thanks very much for pointing out the faults in the supplementary material in the following paragraph. We did the modification and responded to the reviewer's comments point-to-point in the following paragraphs.

Furthermore, the results should be compared to the results of earlier studies where possible. Proper credit is given to earlier studies, but I do not read whether this new study confirms of falsifies results from earlier studies.

Thanks for the comments above. This study confirms the results of earlier studies. We added two sentences to state this consistency in the following.

In line 5, page 20696, we added:

"These seasonal and synoptic effects are very similar to those presented in Peylin et al. (2011) at station scale."

In line 13, page 20696, we added:

"The synoptic-scale impact is comparable to the results in Peylin et al. (2011), which a ~5 ppm effect was found."

The authors should include a brief paragraph that outlines this.

Figure S1 in the appendix seems to show emissions at a time resolution of 3 hours, while the text (page 20684, line 14) mentions hourly time resolution.

We actually downscaled the emissions from a daily total to a three-hour model simulation resolution. We added this statement in the sentence, as follows:

"…and then distributing the daily total according to a three-hour model simulation resolution according to the hourly diurnal fractions from TIMES."

Furthermore, the normalized diurnal cycle of the BLH for the biospheric fluxes (green dashed) pronouncedly differs from the cycles calculated for the three LSRs. This might be due to the sampling of BLH variations at different latitudes or the inadvertent inclusion of oceanic grid boxes. The authors should better analyze and explain this.

Thanks for pointing out the mistake in the BLH. We carefully checked code and found that some oceanic boxes were included when processing the land BLH. We modified the processing code and recalculated the BLH for biospheric fluxes. The corrected BLH is plotted in Figure S1.

Moreover, the mean of the dashed curves to not seems to be produce the expected zero value. The authors should make clear how these curves are calculated and maybe also should produce non-normalized values.

We corrected the normalized value and modified the plots using the correct value in Figure SI.1 and SI.2.

Figure S2 presents daily emission differences (caption mentions emissions). Moreover, the units seem wrong to me since an area unit is missing. Probably the values represent emission units per grid cell. This needs to be corrected.

Yes. The figures show the emissions differences between the weekly-cycle emissions and flat emissions with the unita as per gigatons carbon per grid cell. We corrected the captions and the units in the figure.

Figure S3: here again the mean value seems larger than 1, which is not expected for normalized emissions. As the authors note, the Chinese values seem strange (with a large jump between December and January), and I sincerely question inclusion of the results in the paper. Maybe simply note the inconsistency and refrain from further discussion here?

The unusual seasonal pattern of Chinese FFCO2 emissions is primarily due to the inaccurate energy consumption data, which is not out of the scope for this study and is discussed in the Gregg et al. (2008) paper. Given the fact that this pattern has an effect on the simulated CO2 concentrations, and that this monthly fraction is likely used in inversion studies and forward transport model simulations, we think showing this result in the paper can be helpful and lead researchers to further explore this unusual pattern. We are sure that it will help the community to pay the attention to this unusual pattern, and then solve this problem.

We already corrected the normalization of emissions, and plotted it in Figure S3.

I do not understand the results presented in paragraph 3.5 and presented in figure 5. The Monday values show pronounced negative values right over the source regions. The authors claim that this is due to "downwind transport" of the lower emissions during the weekend, but in my opinion a downwind effect would look rather different. I firmly believe results should look more like figure S2, which shows the underlying emissions. The authors should further scrutinize their implementation of the emissions in the model, and the subsequent analysis ("Monday" sampling is not trivial for models that normally use UTC). Anyhow, the hand-waving argumentation at the end of section 3.5 should be substantiated with further analysis.

Thanks for pointing it out. We totally agree that 'downwind effect' is not an appropriate description of the pattern. The negative values on Monday over the large source regions result mainly from the effect of low weekend emissions that dominate those from large Monday emissions. Thus, it is a residual effect of the low emissions from Saturday and Sunday. We replaced the phrase 'downwind transport' with phrase 'residual effect' in the text. We have modified the sentences of paragraph 3.5 as follows:

“In contrast to other weekdays, Monday shows positive values only in narrow portions of East Asia. The other large source regions show negative surface $FFCO_2$ concentration difference values. This spatial pattern primarily reflects the residual effect of the lower weekend $FFCO_2$ emissions. This coherent $FFCO_2$ concentration difference dissipates after 24 hours and is then dominated by the higher weekday $FFCO_2$ emissions. The residual effect of the larger Friday $FFCO_2$ emissions does not show up in the clearly on thesimulated weekend $FFCO_2$ concentration (Fig. 5d), due to the fact that the weekend mean is constructed from two days and the residual effect from effect from Friday is likely negated in the two day mean.”

Referee #2

This paper uses an atmospheric chemistry transport model for simulating CO2 concentrations due to fossil fuel CO2 emissions at varying time resolution, namely, hourly to annual intervals. The simulation method chosen here is well established and the topic of research is quite relevant for the present day CO2 research. However, this work did not make any effort to analyze the model simulations in comparison with measurements. Thus, I am still wondering which fossil fuel CO2 emission is more close to real world situation? Yes, I agree we should use the time resolved CO2 emissions, but only when we are told that the diurnally varying emissions is correctly modelled. Anyways, the paper is clearly written and may be considered for publication after a revision or sufficient clarifications provided in reply to my comments below.

I do not think the experiments are well thought out. For a fair comparison, you need to first make the DCE FF emissions by including the weekly, daily and diurnal cycle first. Then apply time aggregation to make daily, weekly, and monthly emissions

Here are the steps to follow in my opinion:

1. Make monthly-mean FF emissions (if you are starting with annual mean emissions)
2. Redistribute monthly-mean FF to daily – by linear interpolation or cubit-spline filter. This will be your (1st guess) MCE.
3. WCE: redistribute daily emissions by introducing weekly effect.
4. DCE: insert diurnal cycle to WCE (now at daily time intervals)

Now, the DCE emissions become your 'control' emission scenario. But by introducing the WCE, your daily emissions should have been somewhat perturbed, and monthly-total may not exactly match with that produced in Step #1 (above). Please check.

I got confused because if you started with a daily time interval field, after applying the MCE, you did not need this cubic spline and conservation of mass issue would not arise. I do not understand why you have to apply these divisions.

Thanks for sharing the above thinking. In this study, the distribution starts from annual total emissions and the individual fossil fuel emissions fields are created separately by distributing the annual total to three-hourly model simulation resolution according to the time fraction. This is clearly stated in five paragraphs in page 20684, line 11 to page 20685, line 5, and each paragraph describes the construction of each emissions field, specifically.

We think the division is similar to that suggested by the reviewer. The 'control' emission fields ("all cycle emission" – ACE) is created in the same steps as the reviewer's thoughts. As described in page 20684, we started from distributing the annual total to monthly mean by introducing monthly fraction and cubic-spline filter to avoid discontinuity, then distributed the monthly mean to daily mean by introducing weekly fraction, finally distributed the daily mean to three-hourly model simulation resolution by introducing the hourly fraction. It is right that daily emissions have been perturbed by introducing WCE. However, provided the transport processes are linear and we are considering differences between emissions with/without a particular cycle then the difference between addition of cycles (as we have done) or removal (as proposed by the reviewer) seems small and each choice equally defensible.

Normally the models take fluxes in g/m2/s or equivalent units.

The model used in this study takes the unit g/m2/s as normally for all experiments.

p 20691, line 8: these are all nice discussions. But please clarify the above to exactly prove these are correct. Secondly, the regionally aggregated seasonal cycles should be shown in main paper, e.g., for china, usa, and west Europe also you will learn more if these plots are made for summer (JJA) and winter (DJF) seasons separately.

In above paragraph, we have clearly explained the construction of the emissions fields. We agree to show the aggregated seasonal cycles in main text is helpful to distinguish the difference among the three regions; however, considering that investigation of fossil fuel emissions is not the focus of the study and a total of three cyclic emissions are investigated, we would like to put the plot in "Supplementary material".

Minor comments:

P 20683, line 21: do you need a reference to Kaya identity here?

We have put the reference in the main text.

Kaya, Y. and Yokoburi, K.: Environment, energy, and economy: strategies for sustainability, United Nations Univ. Press., ISBN 9280809113, 1997.

P 20684, line 6: is 'TIMES' an acronym?

Here "TIMES" refers to a data product that generated the diurnal and weekly time cycles of fossil fuel emissions that we have used in this study. We stated this on page 20684, line 6.

P 20686, line 24: do you mean Peylin et al., 2013? Then I think Law et l. (2008) is a better reference here.

We added Law et al. (2008) as a reference in the text and reference section.

P 20687, line 22: is this constant or variable (7.5 being the shortest/longest limit)?

It refers to a constant time step in the model simulation.

We added the word 'constant' in the sentence to illustrate this.

P 20688, line 10: I think globalview-co2 is not an appropriate choice for this analysis. Since your model o/p are at 3-hr intervals and your analysis did not require interpolated data, I would recommend you to sample the model results at the observation time using the real data from WDCGG.

We agree that observations from WDCGG are another option for comparison with the simulated CO_2 concentration. However, given the fact that how time-varying fossil fuel CO_2 emissions affect the estimates of inverse-estimated carbon fluxes is one critical concern for the inversion community, and the globalview-CO_2 are widely used for inversion studies, we are sure that the comparison with the global-CO_2 dataset meets the motivation of this study. Part of the point of the paper is the way the cycles in emissions affect snapshot measurements like flasks.

P 20692, line 5: aren't the tall tower measurements made continuously, shouldn't they be using data at all times?

We agree that the tall towers typically measure the atmospheric CO2 concentration continuously. However, most inversion systems select daytime values given the challenges faced by existing transport models in simulating the stable nocturnal planetary boundary layer.

P 20692, line 21: The widespread negative values may arise from something not properly set in terms of emission as mentioned earlier (experimental design).

The negative values widely appear in small/little emissions, which is mainly due to the residual effect of the difference between the simulated DCE and FE CO_2 emissions. The stable nocturnal planetary boundary layer leads to lower-CO_2 air to the surface in DCE experiment compared to FE experiment, thus, resulting negative values - which continue to exist in these regions until afternoon hours.

We modified the sentence in page 20692, line 11:

"Negative values are present over regions with low emissions, which is mainly due to the interaction of small emissions and a stable PBL at nighttime and the early morning in the DCE experiment compared to the same dynamic FE experiment."

P 20694, line 17: which means the DCE in FF emis leads to deeper seasonal amp in summer? This may imply that we need less biospheric uptake in the summer by inversion. Or if the peak is higher in the winter than we need weaker source by inversion – resulting in stronger biospheric sink regionally.

This is correct. Put another way if part of the amplitude which we normally associate with the biosphere should actually be associated with fossil fuel then fixing this problem should reduce the biospheric amplitude. The key point is that the resulting amplitude change should be small in most places.

P 20695, line 11: but what about the city hotspots? Why aren't those start to appear? Or the –ve values are due to how time is defined. Monday of UTC (model) time is mostly Sunday in California. Is leap-year accounted for properly?

Thanks for the comments. The city hotspots are due mainly to the dominant effect of large emissions on Monday over the residual effect of the weekend. We agree that time definition may introduce uncertainty, especially in eastern Asia and western US (8 hours difference from UTC), but we are sure that the effect is very small after carefully check. Yes, we are sure we accounted leap-year properly.

To more accurately state the effect, we modified the sentence in Page 20695, line 11 in the following:

"This spatial pattern primarily reflects the residual effect of the lower weekend $FFCO_2$ emissions".

P 20695, line 18: sited ✍ situated

We made the change.

P 20697, line 5: straight → simple

We made the change.

P 20697, para 2 : how will then people claim that they can track megacity fossil emission from space. Can you show the mean column averaged CO2 map for one of your simulation – I am curious how elevated the column-CO2 appear due to FF CO2 emissions alone.

We think that the results found here don't conflict with the claim that fossil emissions in megacities can be tracked from space. The following figure maps the column averaged CO_2 concentration by all-time cycle fossil fuel CO_2 emissions. In the figure, the annual mean CO_2 concentration is shown as large as ~13 ppm in megacity of East Asia, Europe and the US.

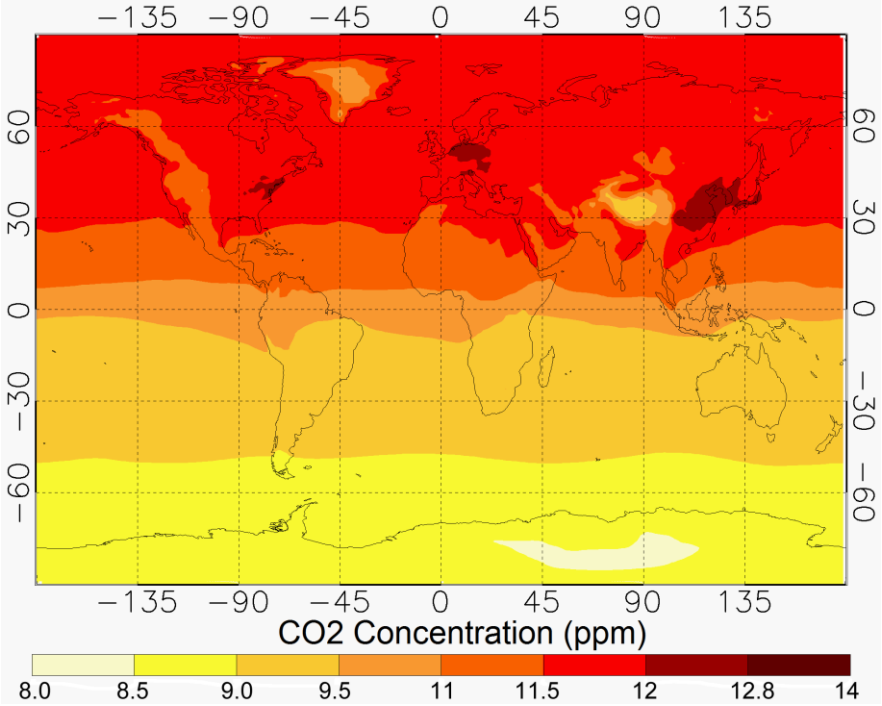

Sensitivity of simulated CO_2 concentration to sub-annual variations in fossil fuel CO_2 emissions

Xia Zhang[1,2], Kevin R. Gurney[1], Peter Rayner[3], David Baker[4], Yu-ping Liu[5]

1.School of Life Science, Arizona State University, Tempe, AZ, United States

2.College of Science, San Diego State University, San Diego, CA, United States

3.Earth Sciences, University of Melbourne, Melbourne, Australia

4.Cooperative Institute for Research in the Atmosphere, Colorado State University, Fort Collins, United States

5.Laboratory for Atmosphere, Science Systems and Applications, Inc., NASA Goddard Space Flight Center Code 614 Greenbelt, United States

Abstract. Recent advances in fossil fuel CO_2 ($FFCO_2$) emission inventories enable sensitivity tests of simulated atmospheric CO_2 concentrations to sub-annual variations in $FFCO_2$ emissions and what this implies for the interpretation of observed CO_2. Six experiments are conducted to investigate the potential impact of three cycles of $FFCO_2$ emission variability (diurnal, weekly and monthly) using a global tracer transport model. Results show an annual $FFCO_2$ rectification varying from -1.35 ppm to +0.13 ppm from the combination of all three cycles. This rectification is driven by a large negative diurnal $FFCO_2$ rectification due to the covariation of diurnal $FFCO_2$ emissions and diurnal vertical mixing, and a smaller positive seasonal $FFCO_2$ rectification driven by the covariation of monthly $FFCO_2$ emissions and monthly atmospheric transport. The diurnal $FFCO_2$ emissions are responsible for a diurnal $FFCO_2$ concentration amplitude of up to 9.12 ppm at the grid cell scale. Similarly, the monthly $FFCO_2$ emissions are responsible for a simulated seasonal CO_2 amplitude of up to 6.11 ppm at the grid cell scale. The impact of the diurnal $FFCO_2$ emissions, when only sampled in the local afternoon is also important, causing an increase of +1.13 ppmv at the grid cell scale. The simulated CO_2 concentration impacts from the diurnally and seasonally-varying $FFCO_2$ emissions are centered over large source regions in the Northern Hemisphere, extending to downwind regions. This study demonstrates the influence of sub-annual variations in $FFCO_2$ emissions on simulated CO_2 concentration and suggests that inversion studies must take account of these variations in the affected regions.

1 Introduction

Quantification of the spatial and temporal distribution of carbon sources and sinks is critical for projecting future atmospheric CO_2 concentrations and climate change (*Field et al,* 2007). Inferring exchanges of CO_2 between the atmosphere and the terrestrial biosphere/ocean from atmospheric CO_2 observations, using inverse methods based on atmospheric transport models, has been an important approach (*e.g., Tans et al.,* 1990; *Enting,* 2002; *Gurney et al.,* 2002). In atmospheric CO_2 inversions, fossil fuel CO_2 ($FFCO_2$) emissions are often treated as a known quantity in the system; consequently, uncertainty in $FFCO_2$ emissions is not considered explicitly and errors in the distribution of simulated atmospheric $FFCO_2$ are translated into errors in the terrestrial biospheric flux estimates. This problem has not been well-studied, due mainly to limitations such as the coarse resolution of traditional $FFCO_2$ inventories, the sparse monitoring of atmospheric CO_2 concentrations, and sub-grid parameterization of atmospheric transport models. In recent years, significant advances have been made in increasing the density of atmospheric observations and in the accuracy, fidelity and resolution of $FFCO_2$ inventories. For example, the network of atmospheric high-frequency CO_2 concentration measurements has grown over the last decade (NACP project in North America and CarboEurope_IP project in Europe). Global $FFCO_2$ inventories have been produced at high resolution in both the space and time domains – these resolve the CO_2 emissions at spatial scales smaller than 10 km and with hourly time resolution (*Rayner et al.,* 2010; *Oda and Maksyutov,* 2011; *Wang et al.,* 2013; *Nassar et al.,* 2013; *Asefi-Najafabady et al.,* 2014). These advances provide information that permits a careful examination of how the high-resolution $FFCO_2$ emission data products impact the spatial and temporal distribution of atmospheric CO_2 and flux estimates (*Ciais et al.,* 2009; *Gurney et al.,* 2005; *Peylin et al.,* 2011; *Nassar et al.,* 2013; *Asefi-Najafabady et al.,* 2014). Further, the development of atmospheric transport models with increased spatial and temporal resolution makes it possible to quantify these impacts (*e.g., Kawa et al.,* 2010; *Peylin et al.,* 2011). Previous literature reported the uncertainty in related inversion and forward simulation studies (*Gurney et al.,* 2005; *Peylin et al.,* 2011; *Nassar et al.,* 2013). For example, Gurney et al. (2005) investigated the impact of monthly-varying $FFCO_2$ emissions on inverted net carbon exchange and found a monthly bias of up to 50% in biospheric net fluxes in some places caused by unaccounted-for variations in fossil fuel emissions. Peylin et al. [2011] showed a seasonal uncertainty of about 2 ppm in simulated CO_2 concentration associated with uncertainty in the

spatial and temporal variability of $FFCO_2$ emissions over Europe. Similarly, Nassar et al. [2013] reported the impact of time-varying $FFCO_2$ emissions on selected geographical regions during wintertime. Previous studies, however, focused on only one or two components of the sub-annual $FFCO_2$ cycles, or else on limited spatial regions or time periods. Thus, a complete exploration of the space/time influence of all sub-annual variations of $FFCO_2$ across the globe is needed.

Inversion analysis infers the distribution of sources and sinks of CO_2 by reconciling the observed global atmospheric CO_2 concentrations at a network of sampling stations with simulated CO_2 concentrations obtained by driving an atmospheric transport model with an initial estimate of CO_2 fluxes. During this process, the interaction of temporally-varying boundary CO_2 fluxes with atmospheric transport/mixing has been shown to impact the inferred surface CO_2 source/sink distribution. For example, the covariation of seasonal/diurnal biospheric fluxes and seasonal/diurnal atmospheric transport causes a significant seasonal/diurnal effect (commonly called the rectifier) on CO_2 concentrations, even if the fluxes at each grid cell average to zero across each time period [*e.g., Keeling et al.,* 1989; *Denning et al.,* 1995, 1996; *Yi et al,* 2004; *Chen et al,* 2004; *Chan et al.,* 2008; *Williams et al.,* 2011]. The biospheric rectification is characterized by a time-mean CO_2 spatial concentration gradient, with the diurnal effect at local-to-regional scales caused by the interaction of diurnal biospheric fluxes with the diurnal variation of vertical mixing in the planetary boundary layer (PBL), and the seasonal rectifier effect at the global scale resulting from the interaction of seasonal biospheric fluxes with seasonal atmospheric transport. By contrast, few studies have quantified the rectification of atmospheric CO_2 concentration associated with the sub-annual variations of $FFCO_2$ fluxes (diurnal, weekly and monthly).

In this paper, we test the sensitivity of simulated global atmospheric CO_2 concentration to sub-annual temporal variations in $FFCO_2$ emissions using a tracer transport model. The sub-annual $FFCO_2$ emission variability is comprised of three cyclic components: diurnal, weekly, and seasonal. The resulting surface atmospheric CO_2 concentration from these individual components and their sum are compared to simulated CO_2 concentrations driven by a "flat" (temporally invariant) $FFCO_2$ emissions inventory. The impact on the column-integral simulated CO_2 concentration is also examined.

The structure of this paper is as follows: Sect. 2 describes the $FFCO_2$ emissions and sub-annual variability, the biospheric fluxes used for comparison with the $FFCO_2$ emissions, the atmospheric tracer transport model employed in model simulations, and the methods for analyzing the model output. In Sect. 3, the results of the flux experiments are presented and discussed at multiple timescales. Section 4 summarizes the results and implications of this study.

2 Methods

In this study, we prescribe five global $FFCO_2$ emission fields that are introduced into the lowest atmospheric layer of a tracer transport model and subsequently run for four simulated years. Three years are considered a spin-up to allow $FFCO_2$ to reach equilibrium through the entire troposphere. The last year is used for analysis and the $FFCO_2$ mixing ratio is analyzed globally and at CO_2 observing sites.

2.1 $FFCO_2$ Emissions

The $FFCO_2$ emissions data product, Fossil Fuel Data Assimilation System (FFDAS) version 2.0, is used as the flux boundary condition for the model simulations in this study (*Asefi-Najafabady et al.*, 2014). The FFDAS $FFCO_2$ emissions were estimated using a diagnostic model (the Kaya identity, *Kaya and Yokoburi, 1997*), constrained by a series of spatially-explicit observational datasets, which decompose emissions into population, economics, energy, and carbon intensity terms (*Rayner et al.*, 2010). The observational datasets used in the FFDAS include a remote sensing-based nighttime lights data product, the Land-Scan gridded population data product, national sector-based fossil fuel CO_2 emissions from the International Energy Agency (IEA), and a recently-constructed database of global power plant CO_2 emissions (*Elvidge et al.*, 2009; *Asefi-Najafabady et al.*, 2014).

The FFDAS emissions are produced at 0.1˚ x 0.1˚ resolution for the years 1997 to 2010. The emissions for year 2002 are used in this study. Sub-annual temporal structure is imposed on these annual emissions based on two additional datasets. Diurnal and weekly cycles are derived from a global data product referred as Temporal Improvements for Modeling Emissions by Scaling ~~(referred as (~~TIMES hereafter) at 0.25˚ x 0.25˚ resolution (*Nassar et al.*, 2013). The monthly temporal cycle is obtained from the global data product developed by Andres et al. (2011) at a resolution of 0.1˚ x 0.1˚ and similarly imposed on the FFDAS emissions. With these temporal structure datasets, five separate $FFCO_2$ emission fields are created:

1) A global 0.1˚ x 0.1˚ $FFCO_2$ emission field in which only the diurnal cycle is represented ("diurnal cycle emissions"-DCE). This is accomplished by distributing the annual emission total in each grid cell evenly for every day of the year (divided by 365) and then distributing the daily total to the three-hour model simulation resolution according to the ~~hourly~~ diurnal fractions from TIMES.
2) A global 0.1˚ x 0.1˚ $FFCO_2$ emissions field in which only the weekly cycle is represented ("weekly cycle emissions"-WCE). This is accomplished by distributing the annual emissions in each grid cell evenly for each week of the year (divided by 52) and then distributing the weekly total according to the day-of-the-week fractions from TIMES.
3) A global 0.1˚ x 0.1˚ $FFCO_2$ emission field in which only the monthly cycle is represented ("monthly cycle emissions"-MCE). This is accomplished by distributing the annual total $FFCO_2$ emissions in each grid cell according to the monthly fractions from Andres et al. (2011). To avoid discontinuities~~y~~ at the month boundaries, a cubic spline filter is applied.
4) A global 0.1˚ x 0.1˚ $FFCO_2$ emission field that represents all of the sub-annual temporal structure ("all cycle emissions"-ACE). This is accomplished by applying the MCE, WCE and DCE fractions in succession with the application of the cubic spline smoother and scaling to ensure conservation of mass.
5) A global 0.1˚ x 0.1˚ $FFCO_2$ emission field with no sub-annual temporal structure ("flat emissions"-FE). Hence, the annual amount in each grid cell is divided by 2920 to obtain evenly distributed emissions at three-hour model resolution.

To understand the temporal variations of the input $FFCO_2$ emission fields used in the simulations, we focus attention on areas of the planet with large $FFCO_2$ emissions, what we refer to as the "large source regions" (LSRs). These regions are located in the U.S. (30˚N to 48˚N, 125˚W to 70˚W), Western Europe (40˚N to 60˚N, 10˚W to 40˚E) and China (20˚N to 45˚N, 105˚E to 125˚E).

The DCE $FFCO_2$ emissions over the three LSRs show a diurnal cycle (supplementary material, Figure SI.1) that is characterized by smaller emissions at night and in the early morning versus larger emissions starting at sunrise and remaining elevated until just after sunset. The DCE emissions typically reach a minimum value between midnight and 3:00 AM and a maximum value at ~15:00 local time. This pattern is expected from the diurnal variations of human activity, such as waking versus sleeping hours and work-related activity cycles (e.g. on-road vehicle "rush"

hours, starting and ending most daily work cycles). We also show the diurnal cycle of planetary boundary layer height used in this study (Fig. S1), which shows similar diurnal variation to the diurnal DCE $FFCO_2$ emissions.

The WCE $FFCO_2$ emissions reflect diminished economic activity on the weekends versus the weekdays. For most of the planet, Saturday and Sunday are the designated weekend days, but in some Middle Eastern countries, Thursday/Friday constitute the weekend days (Fig. S2).

The MCE $FFCO_2$ emissions reflect the different energy needs in winter versus summer: for example, due to space heating of buildings (Fig. S3). However, the space/time patterns reflect different fossil fuel-based energy use across the planet. For example, the $FFCO_2$ emissions in western Europe are larger in December and January and smaller in July and August. The US also shows peak emissions in December-January, but with a second peak in July-August. The summer peak is due to electricity-driven air-conditioning prevalent in the United States [*Gregg et al.*, 2009]. China exhibits an unusual monthly variation, with the largest $FFCO_2$ emissions in December followed by a sudden drop in January and February, and then an increasing trend to December. This has been attributed to uncertainty in the underlying energy consumption data, discussed in detail in Gregg et al. [2008].

To enable atmospheric transport simulation, the five FFDAS emission fields were regridded from their original 0.1˚ x 0.1˚ spatial resolution to the 1.25˚ x 1˚ atmospheric transport model (see Section 2.3) resolution (longitude x latitude). When regridding, emissions originally emanating from land are often allocated to water-covered grid cells – an artifact typically encountered along coastlines when regridding from a fine to coarse resolution. Such a mismatch can lead to a dynamical inconsistency between the emissions and atmospheric transport. To avoid this error, we apply the "shuffling" reallocation method described in Zhang et al. [2014] for all five emissions fields. For the purposes of atmospheric transport simulations, the emissions derived from FFDAS for the year 2002 are repeated across all the years in the atmospheric transport model runs.

2.2 Biospheric fluxes

In order to place the impact of the temporal variation in $FFCO_2$ emissions within a larger context, an additional experiment is conducted driven by terrestrial biospheric carbon fluxes with diurnal and seasonal variations. The biospheric CO_2 flux is a recent version of that used in the TransCom

experiment: CASA model NEE estimates with "neutral" annual fluxes (e.g. *Law, et al., 2008; Peylin*, 2013; *Randerson et al.*, 1997) at a 1˚ x 1˚ spatial resolution and three-hourly temporal resolution (referred as 'CASA fluxes' hereafter). The terrestrial biospheric fluxes have a seasonal cycle, characterized by negative values (carbon uptake from the atmosphere to land) during the growing season (late spring and summer) versus positive fluxes (carbon release from the land to the atmosphere) during the dormant season (winter and early spring) (Fig. S3). The biospheric fluxes also contain diurnal variation with typically negative values during the daytime (dominated by photosynthetic uptake) and positive values during the night (dominated by respiration) (Fig. S1)

The biospheric fluxes are regridded from the original 1˚ x 1˚ to the 1.25˚ x 1˚ transport model resolution with the same shuffling method used for the $FFCO_2$ emission fields.

2.3 Transport model

A global tracer transport model, the Parameterized Chemical Transport Model (PCTM), is used to simulate the $FFCO_2$ concentrations resulting from each of the five $FFCO_2$ emission fields (*Kawa et al.* 2004; 2010). The meteorological fields from the Goddard Earth Observing System Data Assimilation System Version 5 (GEOS-5) MERRA reanalysis products are used to drive the atmospheric transport (*Reineker et al.*, 2008). The model uses a semi-Lagragian advection scheme (*Lin and Rood*, 1996); the subgrid-scale transport includes convection and boundary layer turbulence processes (McGrath-Spangler and Molod, 2014). The model grid is run at 1.25° longitude x 1° latitude with 72 hybrid vertical levels, and produces CO_2 concentration output every hour. The CO_2 concentration output from PCTM has been widely used in comparison with *in situ* and satellite measurements (*Parazoo et al.*, 2012). It has been shown that PCTM simulates the diurnal, synoptic, and seasonal variability of CO_2 concentration well [e.g., *Kawa et al.*, 2004; 2010; *Law et al.*, 2008].

A total of six emission cases are run through the PCTM. The GEOS-5 meteorology has a 3-hour time resolution and a constant 7.5-minute time step is used in the model simulations.

2.4 Analysis methods

In this study, all five $FFCO_2$ simulations use the same meteorology and the same annual total $FFCO_2$ emissions. The only difference between the $FFCO_2$ simulations is the sub-annual temporal structure as described in Sect. 2.1. Hence, the resulting atmospheric $FFCO_2$

concentration differences are due to the differences in the time structure of the $FFCO_2$ emissions only. The atmospheric $FFCO_2$ concentration is examined in two ways: (a) near the surface (at ~998 hPa; in the bottom layer which is ~126 m or ~15 hPa thick) and (b) as a pressure-weighted column integral. In order to understand how the different cyclic components of the $FFCO_2$ emissions interact with the simulated atmospheric transport at multiple time scales, we present the simulated $FFCO_2$ concentration results for the annual mean, and individual sub-annual cycles for both near-surface and column-integral (diurnal, weekly, monthly). In addition to global difference maps, concentration differences between the cyclic and flat $FFCO_2$ emissions are examined at selected GLOBALVIEW-CO_2 monitoring sites (http://www.esrl.noaa.gov/gmd/ccgg/globalview/co2/) (*Masarie and Tans*, 1995).

The impact of the $FFCO_2$ emissions' sub-annual temporal structure is defined as the simulated concentration difference between each sub-annually varying $FFCO_2$ emission field and the FE emission field, when averaged over specific time-cycles:

$$\Delta C_{it} = \frac{1}{N}\sum_{k=1}^{N}\left(\frac{1}{M}\sum_{j=1}^{M} C_{it(j,k)} - \frac{1}{M}\sum_{j=1}^{M} C_{if(j,k)}\right) \quad (1)$$

where ΔC_{it} is the mean concentration difference at the i^{th} grid cell for cyclic emissions, N is the total counts of cycles over the investigated period, $C_{it(j,k)}$ is the j^{th} hourly concentration in the k^{th} cycle at the i^{th} grid cell for cyclic emissions, M is the total counts of hourly periods for each cyclic emissions, $C_{if(j,k)}$ is the j^{th} hourly concentration in the k^{th} cycle at the i^{th} grid cell for flat emissions.

By utilizing Eq. (1), the impact on simulated CO_2 concentration is examined for each individual sub-annual $FFCO_2$ emissions cycle and their combination. Impacts include:

1) The annual mean full-day concentration difference between each cyclic $FFCO_2$ emission and the flat emission fields, in order to explore $FFCO_2$ emissions rectification;
2) The annual mean afternoon (noon to 6 pm local time) concentration difference between the DCE and FE emission fields, to examine the impact at typical atmospheric monitoring times;
3) The annual daily mean concentration difference on weekdays/weekends between the WCE and FE emission fields, to examine the impact of weekly cycles;

4) The diurnal amplitude of hourly mean concentration difference over the year between the DCE and FE emission fields, to examine the impact of diurnal cycles, and
5) The seasonal amplitude of monthly mean concentration difference between MCE and FE emission fields, to examine the impact of the seasonal cycles.

The amplitude of the simulated concentration differences for DCE and the MCE simulations is defined as:

$$C_{amp,it} = C_{max,it}\left\{\Delta C_{itj}|_{j=1,M}\right\} - C_{min,it}\left\{\Delta C_{itj}|_{j=1,M}\right\} \quad (2)$$

where $C_{amp,it}$ is the amplitude at the i^{th} grid cell, $C_{max,it}$ is the maximum of the concentration differences at the i^{th} grid cell, $C_{min,it}$ is the minimum of the concentration differences at the i^{th} grid cell, and $\Delta C_{itj}$is the mean concentration difference for the j^{th} point of the sub-annual cycle at the i^{th} grid cell that is defined as Eq. (1), M is the total points of the sub-annual cycle.

3 Results and discussion

3.1 The $FFCO_2$ rectifier

Figure 1a shows the annual mean full-day surface $FFCO_2$ concentration difference between the ACE and FE emission fields (ACE minus FE). Despite the same annually integrated emissions at each grid cell, the annual mean surface concentration difference shows non-zero values, suggesting rectification of the $FFCO_2$ emissions. The largest negative surface $FFCO_2$ concentration differences (up to -1.35 ppm) are found over the LSRs, coincident with the largest fossil fuel-based industrial activity and energy consumption. Smaller positive surface $FFCO_2$ concentration differences (up to 0.13 ppm) appear over north and northeastern Europe and western Siberia. The annual mean surface $FFCO_2$ concentration difference between the DCE and FE and the MCE and FE are shown in Fig. 1b and 1c, respectively. The negative surface $FFCO_2$ concentration differences in Fig. 1a are primarily driven by the DCE emissions (Fig. 1b) while the positive differences are primarily driven by the MCE emissions (Fig. 1c). Figure 1a includes the contribution from the WCE emissions, but no rectification results from this emission cycle at annual scales (Fig. S4).

Over the LSRs, the diurnal $FFCO_2$ emissions are temporally correlated with the diurnal variation of the PBL (Fig. S1). The emissions are largest during daytime when the PBL is well-mixed, so air with enriched CO_2 tends to be transported aloft. By contrast, the smaller nighttime $FFCO_2$

emissions are mixed into a typically shallower and stable PBL, so this lower-CO_2 air is confined closer to the surface. This covariation, when compared to the same dynamic coupling in the FE field, leads to greater $FFCO_2$ loss from the surface to the free troposphere in the ACE simulation, resulting in the negative annual mean surface $FFCO_2$ concentration difference values over the LSRs. The negative DCE rectification is up to -1.44 ppm at the grid cell scale over the western US (Fig. 1b). Note that the diurnal $FFCO_2$ rectifier effect shows little variation across the LSRs, due mainly to the similar diurnal amplitude of the diurnal emission fields.

The annual mean surface $FFCO_2$ concentration differences between the MCE and flat FE emissions are largest over the LSRs during the local winter months and smallest during the local summer months (Fig. S3). This variation interacts with simultaneous variations in PBL variation. However, distinct from the diurnal $FFCO_2$ rectification, the seasonal $FFCO_2$ rectification shows positive values (up to 0.23 ppm) for north-and-northeastern Europe versus negative values (up to -0.28 ppm) in East Asia, and a near-zero signal (no rectification) in the US (Fig. 1c). The positive rectification obtained in north-and-northeastern Europe to Siberia is associated with the coincidence of large wintertime $FFCO_2$ emissions and weak wintertime atmospheric mixing, which tends to trap CO_2-enriched air near the surface. Additionally, the greater vertical mixing in summertime interacts with the smaller summer $FFCO_2$ emissions, thus, distributing more of the CO_2-depleted air to the free troposphere. The limited seasonal rectification in North America versus the other LSRs is mainly due to the more complex $FFCO_2$ emissions seasonality, with peak emissions in both the winter and summer months as shown previously. Finally, the negative rectification in East Asia is mainly ascribed to the previously mentioned anomalous monthly $FFCO_2$ emissions in China (increasing trend from January to December) and their interaction with atmospheric transport. Hence, the CO_2-depleted air is confined to the surface in East Asia by the very small $FFCO_2$ emissions combined with the inactive atmospheric transport in January and February.

The rectification of the $FFCO_2$ fluxes can be compared to the well-known biosphere flux rectifier. Surface concentration differences of up to 20.35 ppm at the grid cell scale for the biospheric flux simulation (Fig. S5) are centered over the tropical land and northern mid-to-high latitudes with much greater spatial extent than found for either the diurnal or seasonal $FFCO_2$ rectifier. Similar to the $FFCO_2$ rectification, the biospheric rectifier is a combination of diurnal and seasonal rectifications (e.g., *Denning et al., 1995,* 1996; *Yi et al,* 2004; *Chen et al,* 2004; *Chan et al., 2008;*

Williams et al., 2011). For the diurnal biospheric rectification, the daytime net negative CASA fluxes typically coincide with a well-mixed PBL and greater interaction with the free troposphere. At night, this flux is typically reversed and mixed into a shallow PBL, resulting in a positive full-day annual mean surface CO_2 concentration due to the greater loss of CO_2-depleted air during the day. In the case of the seasonal biospheric rectifier, the summer net negative CASA fluxes are mixed into a thicker PBL, resulting in a strong negative surface perturbation, whereas the winter net positive CASA fluxes are mixed into a thinner PBL, resulting in a weaker positive perturbation. The two interactions combine to give a positive annual mean surface CO_2 concentration. The above analysis indicates that $FFCO_2$ rectification is mechanistically similar to biospheric rectification, but the $FFCO_2$ rectifier effect occurs mainly at local-to-regional scales while the biosphere rectification is expressed at a larger spatial scale.

3.2 Impact on afternoon sampling

Atmospheric inversion studies of CO_2 fluxes using flask and tall tower atmospheric CO_2 measurements require consideration of CO_2 concentration sampling times [*e.g. Peters et al., 2007; Dang et al., 2011*]. Given the importance of the simulated CO_2 concentration to the diurnal cycle of $FFCO_2$ emissions, we sub-sample the DCE $FFCO_2$ simulation output for local afternoon (noon – 6 pm) conditions, a common sampling time for flask measurement and a chosen sampling time by inversions to avoid the difficulties associated with capturing nighttime PBL dynamics. Figure 2 presents the spatial distribution of the annual mean, afternoon-only surface $FFCO_2$ concentration difference between the DCE and FE fields. Values vary from -0.21 ppm to +1.13 ppm, with larger positive values centered over the LSRs. Negative values are present over regions with ~~widely shown in~~ low emissions, which is mainly due to the interaction of small emissions and a stable PBL at nighttime and the early morning~~.~~ in the DCE experiment compared to the same dynamic in the FE experiment. The afternoon and 24-h mean signals (Fig. 1b) are of opposite signs but roughly the same magnitude over the LSRs. This is due to the afternoon signal being sampled at the time of the largest afternoon emissions, but also contributing the weakest surface signal to the 24h diurnal span. The afternoon mean signal indicates that a potential bias would be incurred by ignoring the diurnal variability of the $FFCO_2$ emissions. It is noteworthy that the afternoon effect mainly occurs at the local scale, and has a much smaller spatial extent than the full-day diurnal rectification. This indicates that CO_2 monitoring strategies could minimize the effect of the $FFCO_2$ diurnal cycle when using afternoon

measurements and the measurements can be taken close to large source regions for studies influenced by the diurnal cycle.

3.3 Impact of the diurnal amplitude

The continuous atmospheric CO_2 measurements taken by many monitoring stations can see the complete 24 h coverage of atmospheric CO_2 concentration, and can enable the estimate of sub-daily fluxes in inversion studies using these data (e.g., Law et al., 2008). This motivates the examination of the diurnal peak-to-peak amplitude of the simulated concentration, since this parameter includes the overall daily information of the diurnal $FFCO_2$ concentration.

Figure 3a displays the amplitude of the annual mean diurnal surface concentration difference between the DCE and FE fields across the globe. The largest amplitude values are centered over the LSRs with peak-to-peak values reaching 9.12 ppm in western US (-117˚E, 34˚N). Local sunrise is the point when the $FFCO_2$ concentrations reach their greatest difference. At local sunrise, the FE emissions exceed the DCE emissions, which are small prior to the increase of daytime emitting activity (Fig. S1). When combined with the minimum in vertical mixing and a shallow nighttime PBL, the resulting $FFCO_2$ concentration difference is negative (DCE minus FE). Local sunset, by contrast, is the point in the annual mean diurnal cycle where the differences between the DCE and FE fields are at their smallest (Fig. S1) and the DCE emissions exceed those of FE. This combines with the much greater vertical mixing and greater PBL height, and tends to ameliorate the resulting surface $FFCO_2$ concentration difference. Hence, the amplitude difference is driven primarily by the concentration difference at the minima of the diurnal cycle (local sunrise).

To provide context for the magnitude of the $FFCO_2$ diurnal amplitude, the surface $FFCO_2$ DCE concentration amplitude can be compared to that resulting from biosphere fluxes. This is shown in Fig. 3b, where the ratio of $FFCO_2$ amplitude to the total of the $FFCO_2$ and biosphere amplitudes is presented. Averaged over the LSRs, the diurnal amplitude of the annual mean $FFCO_2$ concentration accounts for more than 15% of the total diurnal amplitude, and this ratio rises as high as 87% at the grid cell scale over the LSRs (corresponding to a $FFCO_2$ diurnal amplitude that is 5 ppm larger than the biospheric amplitude, Fig. 3b). The diurnal amplitude can be examined seasonally as well. The diurnal $FFCO_2$ amplitude accounts for a larger portion (up to 5 ppm) of the total diurnal variation than the diurnal biospheric amplitude in winter when the

biosphere is relatively quiescent and vertical mixing is less vigorous (Fig. S6). Overall, this result indicates that studies of diurnal atmospheric CO_2 should consider the contribution of diurnal $FFCO_2$ emissions, especially over LSRs and in wintertime.

3.4 Impact of the seasonal amplitude

Figure 4 shows the amplitude of monthly CO_2 concentration difference between the MCE and FE (MCE- FE) fluxes. The seasonal amplitude varies from 0.01 ppm to 6.11 ppm, with large signals over the LSRs as seen in previous figures. Both the magnitude and spatial extent are larger than found in the diurnal case. The longer periodicity allows more time for an atmospheric signal to build up and to be advected further from the emission source regions. The seasonal maxima and minima contribute equally to the amplitude for all regions (Fig. S7). The seasonal maximum mainly occurs in December-January, driven by the larger $FFCO_2$ emissions during winter (Fig. S8). The seasonal minimum exhibits variable timing across the LSRs, with January for China (up to -3.42 ppm), August/September for the US (-1.09 ppm) and June/July for west Europe (-2.55 ppm). This timing is consistent with the timing of the smallest $FFCO_2$ emissions over each region (Fig. S8). The seasonal minimum in East Asia is, as has been mentioned, likely an artifact of the inventory statistics.

The $FFCO_2$ seasonal amplitude can also be compared to the seasonal biospheric amplitude, for context (Fig. 4b). The biospheric amplitudes are much larger than the $FFCO_2$ amplitudes at the global scale, except for specific industrialized source regions in the US, western Europe and East Asia, where the $FFCO_2$ amplitude accounts for more than 25% of the total seasonal amplitude. This result indicates a non-negligible local-to-regional $FFCO_2$ effect on seasonal amplitude of atmospheric CO_2 concentration.

3.5 Impact of the weekly cycle

The impact of the weekly cycle of $FFCO_2$ emissions is demonstrated here by constructing a mean weekday and mean weekend surface $FFCO_2$ concentration from the difference between the WCE and FE simulations (Fig. 5). As expected, the surface $FFCO_2$ difference values are centered over LSRs, with predominantly positive $FFCO_2$ concentration values for the weekdays and negative values on the weekends. The negative weekend values are a reflection of the reduced weekend $FFCO_2$ emissions versus weekday activity (*Nassar et al.,* 2013). There are a few deviations from this regular weekday/weekend pattern. First, the different definition of what constitutes weekend

activity is seen over the Middle East, where the weekend is typically Thursday-Friday versus Saturday-Sunday in most of the rest of the world. In contrast to other weekdays, Monday shows positive values only in narrow portions of East Asia. The other large source regions show negative surface $FFCO_2$ concentration difference values. This spatial pattern primarily reflects results ~~mainly from~~ the residual effect ~~downwind transport~~ of the lower weekend $FFCO_2$ emissions. This coherent $FFCO_2$ concentration difference dissipates after 24 hours and is then dominated by the higher weekday $FFCO_2$ emissions. The residual effect~~downwind transport~~ of the larger Friday $FFCO_2$ emissions does not show up in the ~~in the isn't shown~~ clearly on the simulated weekend $FFCO_2$ concentration (Fig. 5d), due to the fact that the weekend mean is constructed from two days and the residual effect from effect from Friday is likely negated in the two day mean ~~.mainly to the dominant effect of the lower weekend emissions~~.

3.6 Sampling at monitoring stations

Atmospheric CO_2 monitoring locations were originally situated away from fossil fuel source regions, but as $FFCO_2$ emissions have risen dramatically over time, they are increasingly influenced by $FFCO_2$ sources. A large number of monitoring stations are situated in strongly affected areas in temperate North America, Western Europe and East Asia that show a strong diurnal concentration. Noteworthy are the coastal sites close to the large source regions in the US and Western Europe – these show significant influence from the DCE flux component, despite the fact that these locations are assumed to represent upwind background CO_2. Timeseries of daily afternoon-mean CO_2 concentration differences demonstrate this influence (Fig. 6). For the sake of brevity, we focus on two stations: La Jolla, in the western US (32.9°N, 117.3°W, 10 m, referred as LJO) and Lutjewad of the Netherlands (53.4°N, 6.35°E, 61 m, referred as LUTDTA). The two sites were selected because they are close to LSRs (locations highlighted in the figure). A strong seasonality of up to 5 ppm for LUTDTA and up to 3 ppm for LJO is shown in the daily afternoon mean CO_2 concentration difference from the ACE simulation. Synoptic variability with approximately the same magnitude is also evident (Fig. 6b). These seasonal and synoptic effects are very similar to those presented in Peylin et al. (2011) at the station scale. Finally, a slight weekly cycle can be seen in spring and summer at both stations.

The timeseries can be further understood through examination of the cyclic $FFCO_2$ flux contributions (Fig. 6c-e). The MCE simulation shows the largest daily afternoon mean impact on

CO_2 concentrations (up to 5.5 ppm) versus smaller values for the WCE (2.2 ppm) and DCE (1.6 ppm). Large seasonality is shown in the MCE that is caused by the interaction of the monthly $FFCO_2$ emissions and atmospheric transport. The WCE and DCE display slight but evident seasonality that is driven mainly by the seasonal atmospheric transport. Synoptic variability is seen in the MCE (up to 4 ppm) and DCE (up to 1 ppm)~~.~~. The synoptic-scale effect is comparable to the results found in Peylin et al. (2011), where a ~ 5 ppm effect was found. Also, a weekly cycle is illustrated for the WCE driven by the weekly $FFCO_2$ emissions. These temporal patterns are common to the stations with significant response to the time-cycle $FFCO_2$ emissions, but the magnitude is dependent on the local dynamical conditions, transport patterns and proximity of the site to the $FFCO_2$ sources. LJO shows a larger impact than LUTDTA in July and August, associated mainly with the large $FFCO_2$ emissions in summer. Differences are found in the timing of the synoptic events between the two sites, and the amplitude of the synoptic variation in the CO_2 concentration difference at LUTDTA is roughly twice that at LJO, which suggests that the synoptic events of atmospheric transport play an important role in distributing the $FFCO_2$ at LUTDTA.

3.7 Column-average concentration

The analysis above indicates significant CO_2 concentration response to sub-annual $FFCO_2$ emission variability near the surface. With the advent of satellite measurements, as well as the surface-based spectrometers of the TCCON network, it is important to examine the response of vertically-average CO_2 concentrations to the $FFCO_2$ emissions. How important is sub-annual $FFCO_2$ emission variability to the CO_2 concentration seen from space? And what impact do these $FFCO_2$ emission cycles have on studies that use satellite measurements?

To answer these questions, the same analysis is performed for the simulated column-integral CO_2 concentration for all the cyclic $FFCO_2$ emissions as was performed for the surface. For generality, we have used simple~~traight~~ pressure weighting to compute the column averages, rather than use the vertical weighting appropriate for any particular satellite. Results indicate weak rectifier effects in the simulated column-integral $FFCO_2$ concentration, with ACE having negative values from -0.02 ppm to -0.06 ppm. The ACE rectification is centered over large source regions and the MCE component represents the largest contribution overall; varying from -0.02 ppm to -0.06 ppm (Fig. S9). The DCE exhibits similar rectification magnitudes varying from -0.02 ppm to -0.04 ppm, but with a response covering a smaller spatial extent. The MCE rectification reflects

the larger vertical and spatial effect of the monthly $FFCO_2$ emission variability as compared to the WCE and DCE. Compared to the surface effect, the column-integral rectification is almost an order of magnitude smaller. However, note the negative signal in west Europe from MCE, which is opposite to the positive signal at the surface (Fig. 1). Overall, the sub-annual $FFCO_2$ emission variability has little effect on all aspects of the column-integral CO_2 concentration.

4 Conclusions and implication

This study investigates the impact of sub-annual $FFCO_2$ emissions cycles (diurnal, weekly and monthly) on the simulated CO_2 concentration. The simulated CO_2 concentrations are examined at multiple time scales over the globe as well as at GlobalView monitoring stations. When expressed as annual means, a $FFCO_2$ rectifier effect is found from the combination of all cycles, which varies from -1.35 to +0.13 ppm, centered over large source regions in the northern hemisphere. This is driven by a large negative diurnal $FFCO_2$ rectification due to the interaction of large/smaller $FFCO_2$ emissions with vigorous/inactive PBL mixing in the daytime/nighttime, and a positive seasonal rectification in Western Europe resulting from the covariance of small/larger $FFCO_2$ emissions in the summertime/wintertime with vigorous/inactive atmospheric transport.

The diurnal $FFCO_2$ emissions are also found to significantly affect the diurnal variation of simulated CO_2 concentrations at the local/regional scale, driven by the covariance of diurnally-varying $FFCO_2$ emissions and vertical mixing. The impact on the diurnal peak-to-peak amplitude is up to 9.12 ppm while the impact on the afternoon mean concentration is as large as +1.13 ppm at the grid cell scale. The results indicate the importance of proper temporal sampling when using/interpreting measurements affected by diurnal $FFCO_2$ emissions (especially those near emission regions). The small spatial extent of the afternoon effect suggests that measurements can be taken close to the large source regions when required for studies that use the afternoon-only measurements.

The monthly $FFCO_2$ variability results in a simulated CO_2 concentration seasonal amplitude (up to 6.11 ppm) over large source regions, caused mainly by the interaction of large/smaller $FFCO_2$ emissions in wintertime/summertime with inactive/vigorous PBL mixing. Significant spatial patterns are found at the regional scale, due mainly to the large difference in the seasonal variations of $FFCO_2$ emissions across the regions. This result suggests that attention should be

given to accurate representation of seasonal profiles of regional emission inventories, particularly for large emitters like China. The diurnal response has a more limited spatial extent than the monthly response and can probably be disregarded when considering clean air oceanic sites.

The simulated CO_2 concentration at the GlobalView stations are found to be affected by all sub-annual $FFCO_2$ cycles, especially for sites close to large source regions. These impacts cover multiple time-scales, from diurnal to seasonal, caused by the interaction/combination of the variable $FFCO_2$ emissions with atmospheric transport. This finding, together with the above, indicates that current inversion studies that do not incorporate sub-annually varying $FFCO_2$ emissions could result in biased flux estimates results due to the $FFCO_2$ rectifier, and that caution should be taken regarding sampling time and when choosing the locations for new sites of atmospheric CO_2 measurement.

Characterization of the column-average simulated CO_2 concentration suggests a weak impact compared to the surface signal, indicating less importance than for surface measurements. This also suggests that including the sub-annual cycles of $FFCO_2$ variability is not as important a concern for modeling studies using only satellite measurements.

Supplementary Information related to this article is available online at doi:10.5194/acpd-15-20679-2015-supplement.

Acknowledgements

This work was supported by the National Science Foundation CAREER award 0846358 and NASA ROSES grant NNX11AH86G. Rayner is supported by an Australian Professorial Fellowship (DP1096309).

References

Andres, R. J., Gregg, J. S., Losey, L., Marland, G. and Boden, T. A.: Monthly , global emissions of carbon dioxide from fossil fuel consumption, Tellus, 63B, 309-327, 2011.

Asefi-Najafabady, S., Rayner, S. P. J., Gurney, K. R., McRobert, K. R. A., Song, Y., Coltin, K., Huang, J., Elvidge, C., and Baugh, K.: A multiyear, global gridded fossil fuel CO_2 emissions data product: Evaluation and analysis of results, J. Geophys. Res., Atmos, 119, 10213-10231, doi:10.1002/2013JD021296, 2014.

Chan, D., Ishizawa, M., Higuchi, K., Maksyutov, S., and Chen J.:Seasonal CO_2 rectifier effect and large-scale extratropical atmospheric transport, J. Geophys. Res., Atm, 113, D17309, doi:10.1029/2007JD009443, 2008.

Chen, B. and Chen, J. M.: A vertical diffusion scheme to estimate the atmospheric rectifier effect, J. Geophys. Res., 109, D04306, doi:10.1029/2003JD003925, 2004.

Ciais, P., J., Paris, D., Marland, G., Peylin, P., Piao, S. L. , Levin, I., Pregger, T., Scholz, Y., Friedrich, R., Rivier, L., Houwelling, S., Schulze, E. D., and members of the CARBOEUROPE Synthesis Team (1):The European carbon balance revisited. Part 1: fossil fuel emissions, Global Change Biol., 16, 1395-1408, doi:10.1111/j.1365-2486.2009.02098.x., 2009.

Dang, X., Lai, C-T., Hollinger, D. Y., Schauer, A. J., Xiao, J., Munger, J. W., Owensby, C. and Ehleringer, J. R.: Combining tower mixing ratio and community model data to estimate regional-scale net ecosystem carbon exchange by boundary layer inversion over four flux twoers in the United States, J. Geophys. Res., 116, G03036, doi:10.1029/2010JG001554, 2011.

Denning, A. S., Fung, I. Y., and Randall, D. A.: Lantitudinal gradient of atmospheric CO_2 due to seasonal exchange with land biota, Nature, 376, 240-243, 1995.

Denning, A. S., Collatz, G. J., Zhang, C., Randall, D. A., Berry, J. A., Sellers, P. J., Colello, G. D., and Dazlich, D. A.: Simulations of terrestrial carbon metabolism and atmospheric CO_2 in a general circulation model. Part 2: simulated CO_2 concentrations, Tellus, 48B, 543-567, 1996.

Elvidge, C. D., Ziskin, D., Baugh, K. E. Tuttle, B. T., Ghosh, T., Pack, D. W., Erwin, E. H., and Zhizhin, M.: (2009), A Fifteen Year Record of Global Natural Gas Flaring Derived from Satellite Data, Energies, 2 (3), 595-622, 2009.

Enting, I.: Inverse Problems in Atmospheric Constituent Transport, Cambridge Univ. Press, New York, 2002.

Field, C. B., Lobell, D. B., Peters, H. A., and Chiariello, N. R.: Feedbacks of terrestrial ecosystems to climate change, Annu. Rev. Environ. Reour., 32, 1-29, doi:10.1146/annurev.energy.32.053006. 141119, 2007.

Gregg, J. S., Andres, R. J., and Marland, G.: China: emissions pattern of the world leader in CO_2 emissions from fossil fuel consumption and cement production. Geophys. Res. Let. 35. L08806, doi:10.1029/2007GL032887, 2008.

Gregg, J. S., Losey, L. M., Andres, R. J., Blasing, G. J., and Marland, G.: The temporal and spatial distribution of carbon dioxide emissions from fossil-fuel use in North America, J. Appl. Meteorol. Climatol, 48, 2528-2542, doi:10.1175/2009JAMC2115.1, 2009.

Gurney, K. R., Law, R. M., Denning, A. S., Rayner, P. J., Baker, D., Bousquet, P., Bruhwiler, L., Chen, Y.-H., Ciais, P., Fan, S., Fung, I. Y., Gloor, M., Heimann, M., Higuchi, K., John, J., Maki, T., Maksyutov, S., Masarie, K., Peylin, P., Prather, M., Pak, B. C., Randerson, J., Sarmiento, J., Taguchi, S., Takahashi, T., and Yuen, C.-W.: Towards robust regional estimates of CO_2 sources and sinks using atmospheric transport models, Nature, 415, 626-630, 2002.

Gurney, K. R., Chen, Y., Maki, T., Kawa, S. R., Andrews, A., and Zhu, Z.: Sensitivity of atmospheric CO_2 inversions to seasonal and interannual variations in fossil fuel emissions, J. Geophys. Res., 110,d10308, doi:10.1029/2004JD005373, 2005.

Kaya, Y. and Yokoburi, K.: Environment, energy, and economy: strategies for sustainability, United Nations Univ. Press., ISBN 9280809113, 1997.

Keeling, C. D., Bacastow, R. B., Carter, A. F., Piper, S. C., Whorf, T. P., Heimann, M., Mook, W. G., and Roeloffzen, H.: A three-dimensional model of atmospheric CO_2 trasport based on observed winds. 1: Analysis of observed data, in Aspects of Climate Variability in the Pacific and Western Americas, Geophys. Monogr. Ser., vol. 55, edited by D. H. Peterson, PP. 165-236, AGU. Washington, D. C, 1989.

Kawa, S. R., Erickson, D. J. III., Pawson, S., Zhu, Z.: Global CO_2 transport simulations using meteorological data from the NASA data assimilation system, J. Geophys. Res., 109, D18312, doi:10.1029/2004JD004554, 2004.

Kawa, S. R., Mao, J., Abshire, J. B., Collatz, G., and Weaver, C. J.: Simulation studies for a space-based CO_2 lidar mission, Tellus, 62B, 759-769, 2010.

Law, R. M., Peters, W., Rödenbeck, C., Aulagnier, C., Baker, I., Bergmann, D. J., Bousquet, P., Brandt, J., Bruhwiler, L., Cameron-Smith, P. J., Christensen, J. H., Delage, F., Denning, A. S., Fan, S., Geels, C., Houweling, S., Imasu, R., Karstens, U., Kawa, S. R., Kleist, J., Krol, M. C., Lin, S.-J., Lokupitiya, R., Maki, T., Maksyutov, S., Niwa, Y., Onishi, R., Parazoo, N., Patra, P. K., Pieterse, G., Rivier, L., Satoh, M., Serrar, S., Taguchi, S., Takigawa, M., Vautard, R., Vermeulen, A. T., and Zhu, Z.: TransCom model simulations of hourly atmospheric CO2: Experimental overview and diurnal cycle results for 2002, Global Biogeochem. Cy., 22, GB3009, doi:10.1029/2007GB003050, 2008.

McGrath-Spangler, E. L., and Molod, A.: Comparison of GEOS-5 AGCM planetary boundary 5 layer depths computed with various definitions, Atmos. Chem. Phys., 14, 6717-6727, 2014.

Masarie, K.A., Tans, P. P.: Extension and Integration of Atmospheric Carbon Dioxide Data into a Globally Consistent Measurement Record. J. Geophys. Res., 100, No. D6, p. 11593-11610, 1995.

Nassar, R., Napier-Linton, L., Gurney, K. R., Andres, R. J., Oda, T., Vogel, F. R., and Deng, F.: Improving the temporal and spatial distribution of CO_2 emissions from global fossil fuel emission data sets, J. Geophys. Res., Atm, 118, 917-933, 2013.

Parazoo, N. C., Denning, A. S., Kawa, S. R., Pawson, S., and Lokupitiya, R.: CO_2 flux estimation errors associated with moist atmospheric processes, *Atmos. Chem. Phys.*, *12*, 6405-6416, 2012.

Peylin, P., Houweling, S., Krol, M. C., Karstens, U., Rödenbeck, C., Geels, C., Vermeulen, A., Badawy, B., Aulagnier, C., Pregger, T., Delage, F., Pieterse, G., Ciais, P., and Heimann, M.: Importance of fossil fuel emission uncertainties over Europe for CO_2 modeling: model intercomparison, Atmos. Chem. Phys., 11, 6607-6622, 2011.

Peters, W., Jacobson, A. R., Sweeney, C., Andrews, A. E., Conway, T. J., Masarle, K., Miller, J. B., Bruhwiler, L. M. P., Pėtron, G., Hirsch, A. I., Worthy, D. E. J., vander Werf, G. R., Randerson, J. T., Wennberg, P. O., Krol, M. C., and Tans, P. P.: An atmospheric perspective on North American carbon dioxide exchange: CarbonTracker, PNAS, 104, 18925-18930, 2007.

Peylin, P., Law, R. M., Gurney, K. R., Chevallier, F., Jacobson, A. R., Maki, T., Niwa, Y., Patra, P. K., Peters, W., Rayner, P. J., Rodenbeck, C., van der Laan-Luijkx, I. T., and Zhang, X.: Global atmospheric carbon budget: results from an ensemble of atmospheric CO_2 inversions, Biogeosicences, 10, 6699-6720, 2013.

Rayner, P. J., Raupach, M. R., Paget, M., Peylin, P., and Koffi, E.: A new global gridded data set of CO_2 emissions from fossil fuel combustion: Methodology and evaluation, J. Geophys. Res., 115, D19306, doi:10.1029/2009JD013439, 2010.

Reineker, M.M., Suarez, M. J., Todling, R., Bacmeister, J., Takacs, L., Liu, H.-C., Gu, W., Sienkiewicz, M., Koster, R. D., Gelaro, R., Stajner, I., and Nielsen, J. E.: The GEOS-5 Data Assimilation System - Documentation of Versions 5.0.1, 5.1.0, and 5.2.0, NASA Technical Report Series on Global Modeling and Data Assimilation, V27, 2008.

Tans, P. P., Fung, I. Y., and Takahashi, T.: Observational constraints on the global atmospheric CO_2 budget, Science 247, 1431-1438, 1990.

Williams, I. N., Riley, W. J., Torn, M. S., Berry, J. A., and Biraud, S. C.: Using boundary layer equilibrium to reduce uncertainties in transport models and CO_2 flux inversions. Atmos. Chem. Phys., 11, 9631-9641, 2011.

Yi, C., Davis, K. J., Bakwin, P. S., Denning, A. S., Zhang, N., Desai, A., Lin, J. C., and Gerbig, C.: Observed covariance between ecosystem carbon exchange and atmospheric boundary layer dynamics at a site in northern Wisconsin, J. Geophys. Res., 109, D08302, doi:10.1029/2003JD004164, 2004.

Zhang, X., Gurney, K. R., Rayner, P. J., Liu, Y., and Asefi-Najafabady, S.: Sensitivity of simulated CO_2 concentration to regridding of global fossil fuel CO_2 emissions, Geosci. Model Dev., 7, 2867-2874, doi:10.5194/gmd-7-2867-2014, 2014.

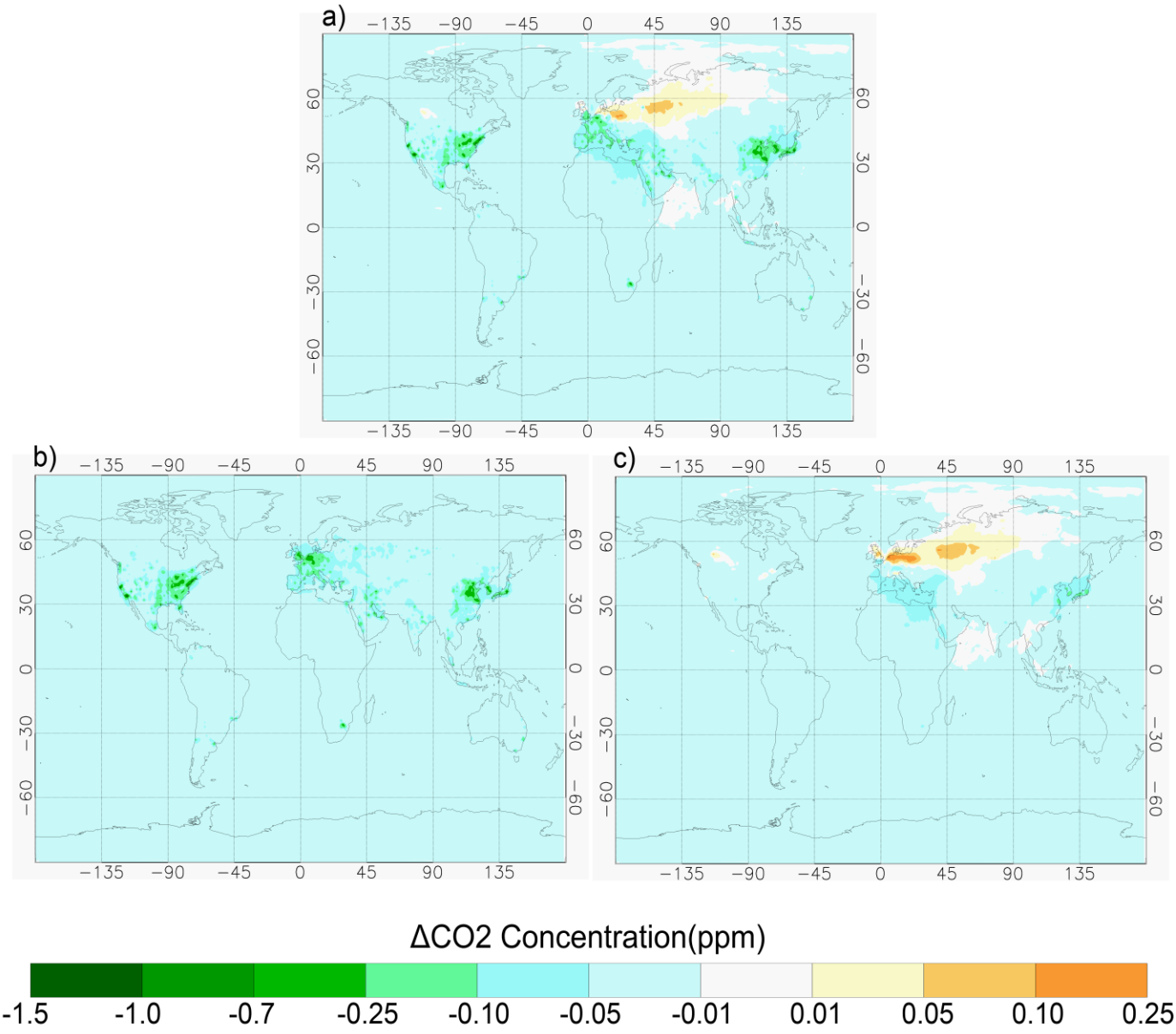

Figure 1. Simulated full-day annual mean surface $FFCO_2$ concentration difference between the time-varying and flat $FFCO_2$ emission fields. a) ACE minus FE; b) DCE minus FE; c) MCE minus FE.

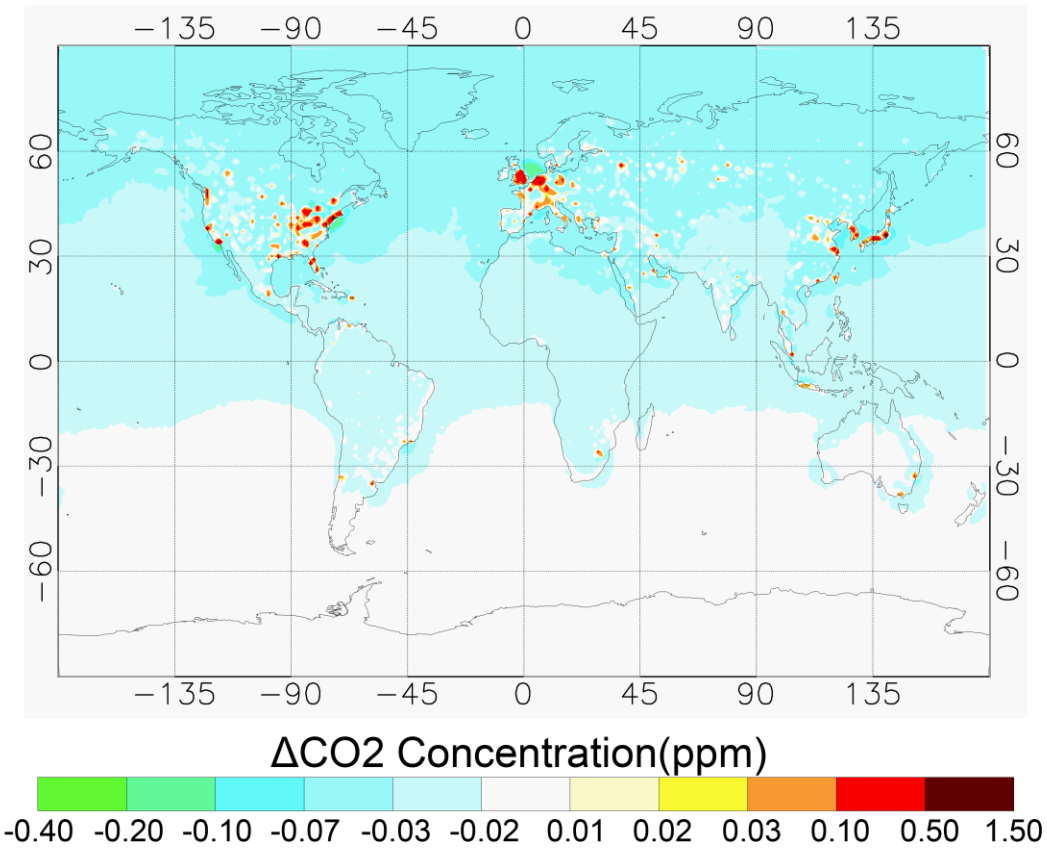

Figure 2. Simulated annual mean surface $FFCO_2$ concentration difference between the DCE and FE $FFCO_2$ emission fields (DCE minus FE), sampled during the local afternoon (12:00 – 18:00).

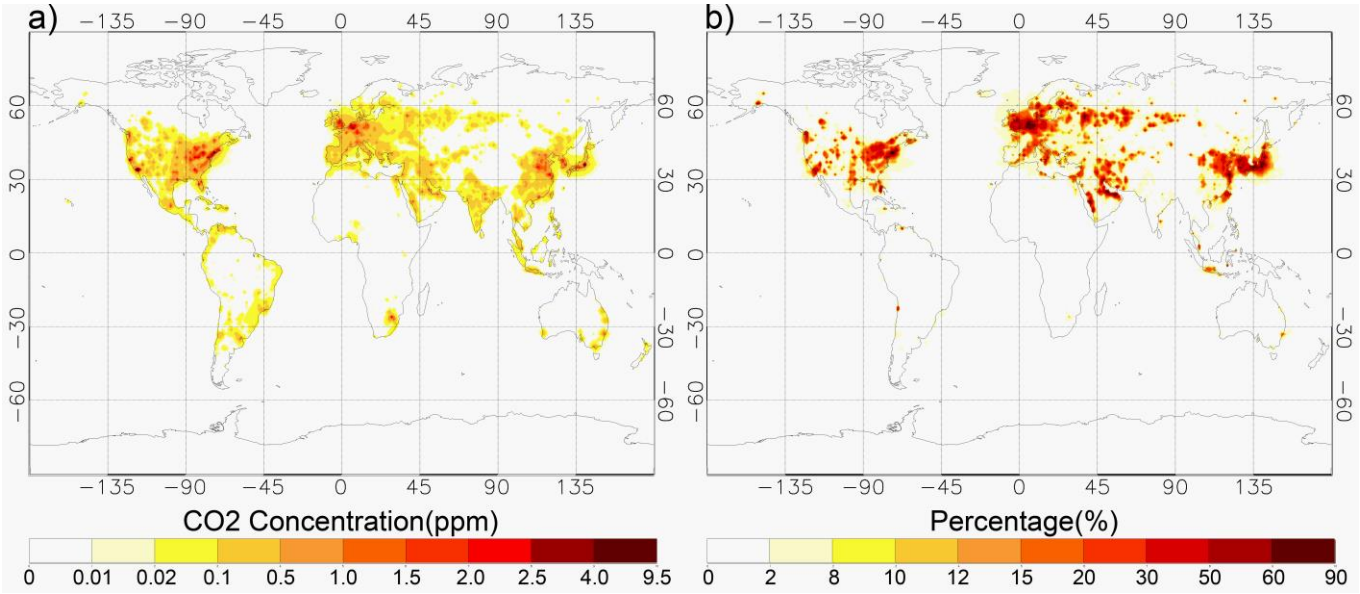

Figure 3. The diurnal amplitude of the $FFCO_2$ surface concentration from the DCE simulation. a) the peak-to-peak diurnal amplitude of the annual mean, hourly concentration difference between the DCE and FE emission fields (DCE minus FE); b) ratio of $FFCO_2$ diurnal amplitude to the diurnal CO_2 amplitude of total $FFCO_2$ and biosphere.

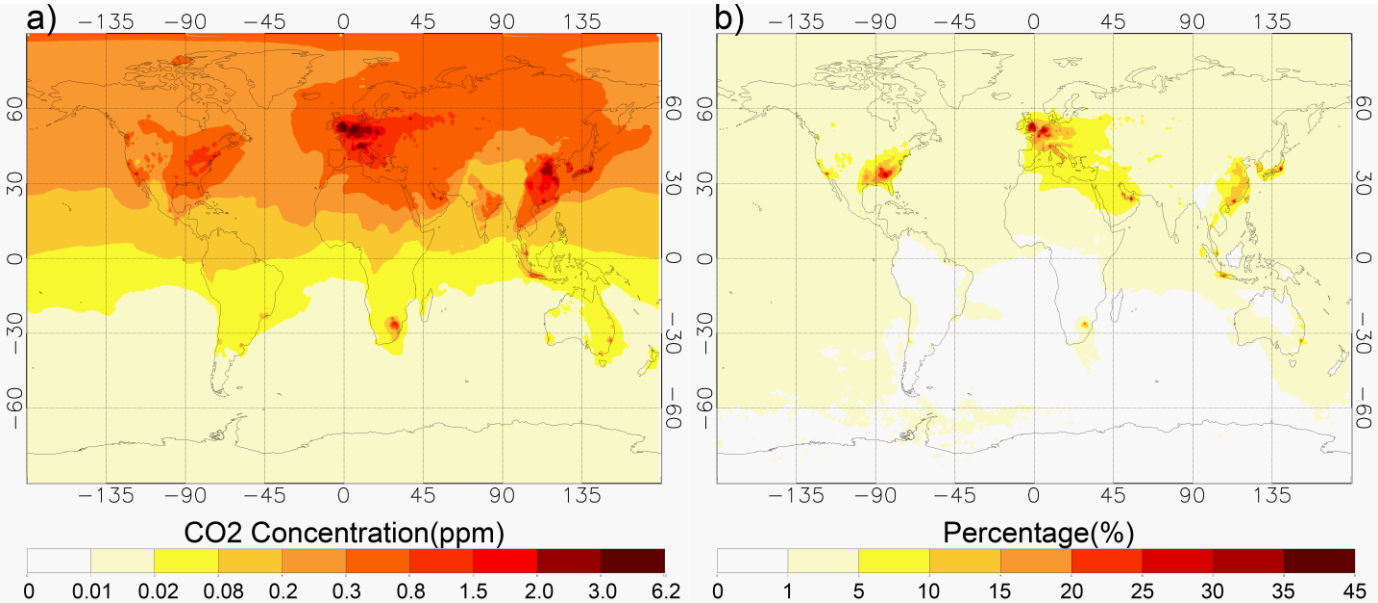

Figure 4. Seasonal amplitude of the simulated surface $FFCO_2$ concentration; a) peak-to-peak seasonal amplitude of simulated surface $FFCO_2$ concentration difference between the MCE and FE emission fields (MCE minus FE); b) ratio of $FFCO_2$ seasonal amplitude to the sum of the $FFCO_2$ and biosphere seasonal amplitude.

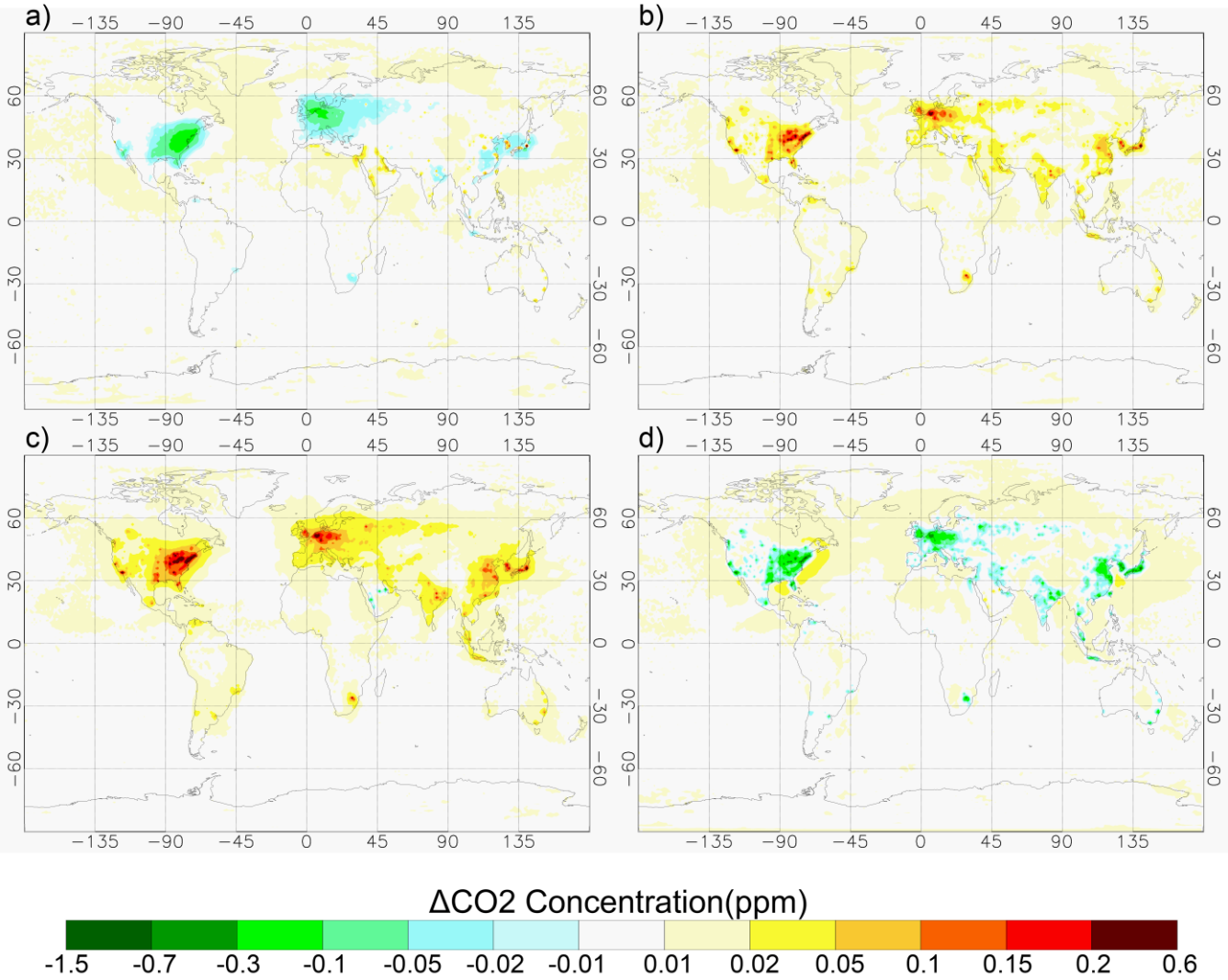

Figure 5. Simulated daily mean surface $FFCO_2$ concentration differences between the WCE and FE emission fields. (a) Monday; (b) Tuesday and Wednesday; (c) Thursday and Friday; (d) Saturday and Sunday.

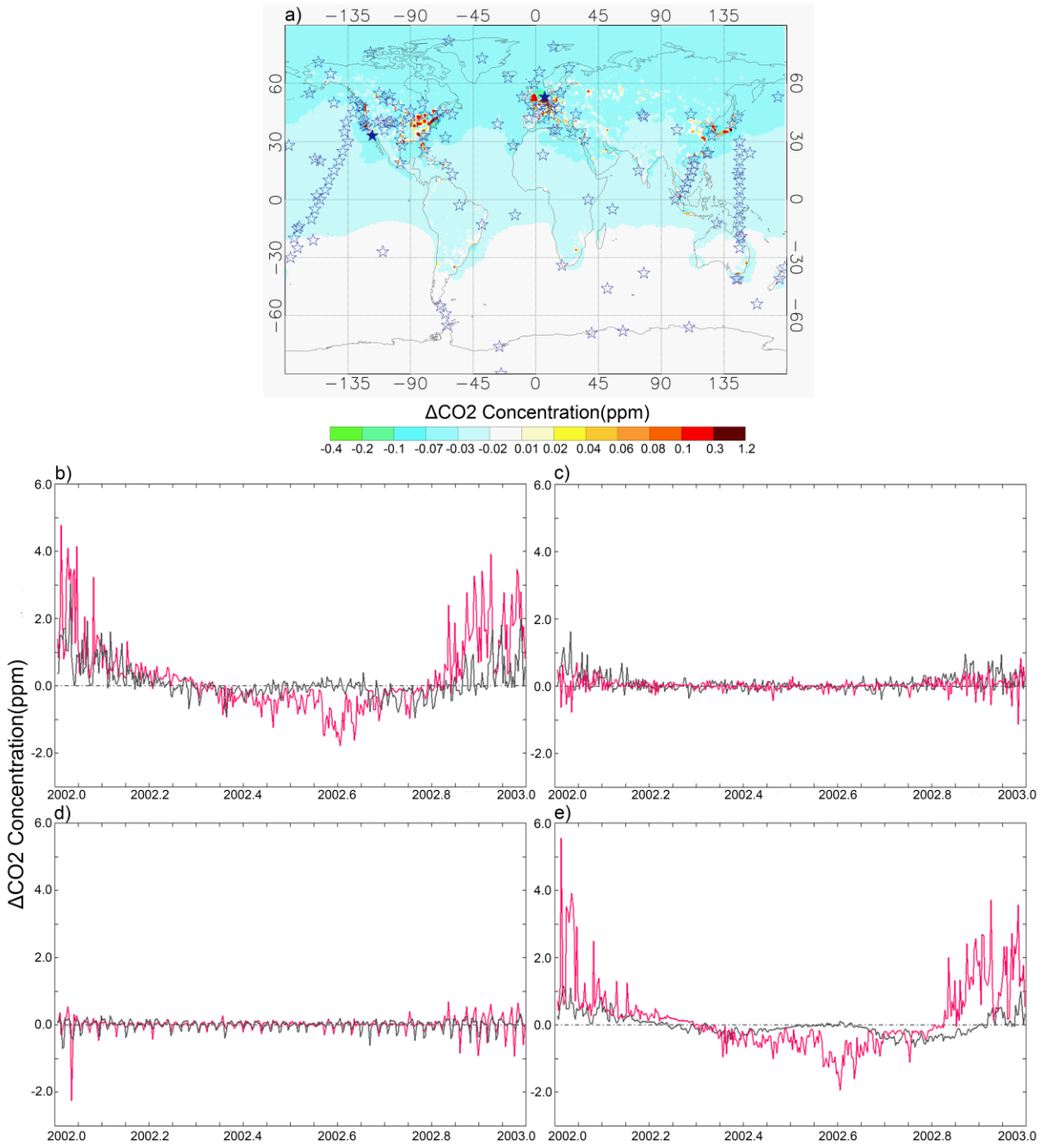

Figure 6. The simulated surface afternoon mean $FFCO_2$ concentration difference (12:00 – 18:00) between the DCE and FE $FFCO_2$ emissions, and the locations of GlobalView monitoring stations (stars). (a) daily afternoon mean $FFCO_2$ concentration differences between each cyclic $FFCO_2$ emissions field and FE emissions at two selected GlobalView stations (LJO – gray; LUTDTA – pink); (b) for all-time cycle emissions, (c) for diurnal-only time cycle emission, (d) for weekly-only time cycle emissions and (e) for monthly-only time cycle emissions. Solid stars indicate the location of LJO and LUTDTA.